Contact Mechanics and Aspects of Polymer Science

Table of Contents:

1. Contact Mechanics – Fully Elastic Models

Hertz analyzed the stresses at the contact of two elastic solids, and thereby assumed small strains within the elastic limit. The contact radius a is considered significantly smaller than the radius of curvature R, and the two contacting surfaces, as depicted in Figure 1, assumed to be non-conformal. Furthermore, creep at the interface is neglected; i.e., a frictionless contact assumed.

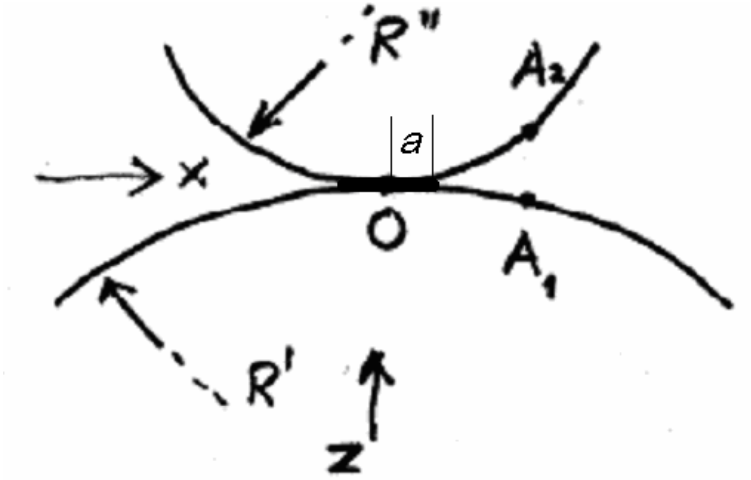

Figure 1: Contact of two elastic spheres.

Based on this assumption, the contact radius a, the contact area A, and both the maximum pressure p_{max} and the mean pressure p_m can be determined with an elastic infinite half-space analysis as:

Hertz contact radius: $a = \left[\frac{3LR}{4E^*}\right]^{1/3}$

Hertz area of contact: $A = \pi a^2 = \pi\left[\frac{3LR}{4E^*}\right]^{2/3}$

Mutual approach: $\delta = \frac{a^2}{R}\left[1 - \frac{2}{3}\left(\frac{a_o}{a}\right)^{3/2}\right]$ with $a_o = a\big|_{L=0}$

Hertz pressure: $p_{max} = \frac{3L}{2\pi a^2} = \frac{3}{2}p_m\left[\frac{6L\left(E^*\right)^2}{\pi^3 R^2}\right]^{1/3}$

with the applied normal force (load) L, and the combined Young's modulus and radius of curvature of the two materials (1 and 2), i.e.,

$$E^* = \left(\frac{1-\nu_1^2}{E_1} + \frac{1-\nu_2^2}{E_2}\right)^{-1} \text{ and } R = \left(\frac{1}{R_1} + \frac{1}{R_2}\right)^{-1}$$

where ν is the Poisson ratio ($\nu \approx 0.5$ for polymers). Neglected in the Hertz model are adhesive interactions, as seen at zero loads where the contact area vanishes.

The adhesion force between two rigid spheres can be expressed as

$$F_{adh} = -2\pi R^* \Delta\gamma; \quad \Delta\gamma = \gamma_1 + \gamma_2 - \gamma_{12}$$

where $\Delta\gamma$ is called the "work of adhesion" per unit area. This force-adhesion relationship is named after *Bradley*. Neither elastic nor plastic deformations are considered in Bradley's model. Johnson, Kendal and Roberts introduced a very successful elastic model - named JKR model. Based on this model, the area of contact $A = \pi a^2$ can be easily deduced from the JKR contact radius, i.e.,

$$a = \left[\frac{3R}{4E^*}\left(L + 3\pi R\Delta\gamma + \sqrt{6\pi R\Delta\gamma L + \left(3\pi R\Delta\gamma\right)^2}\right)\right]^{1/3}.$$

Note, for vanishing work of adhesion, the JKR expression for a corresponds to the Hertzian contact radius. For non-zero adhesion forces, the significant difference of the two models is illustrated in Figure 2. With the JKR model, a negative loading regime between L = 0 and the instability load, i.e., the adhesion force

$$L = F_{adh}{}^{JKR} = -\frac{3}{2}\pi R^* \Delta\gamma \text{, is possible.}$$

Considering that the JKR adhesion force equation is seemingly independent of any elastic modulus, there seems to be an inconsistency, if compared to the Bradley model above. The apparent discrepancy was resolved by David Tabor (1977) who introduced the following parameter:

$$\mu = \frac{\left(R^*\right)^{1/3}(\Delta\gamma)^{2/3}}{\sigma\left(E^*\right)^{2/3}}, \qquad \textit{"Tabor Coefficient"}$$

where E^* and R^* are the combined curvature and modulus, respectively, and σ the characteristic atom-atom distance. The Tabor coefficient μ expresses the relative

importance of the adhesive interaction versus the elastic deformation. For $\mu > 5$, which is typical for soft organic materials, the JKR model is appropriate.

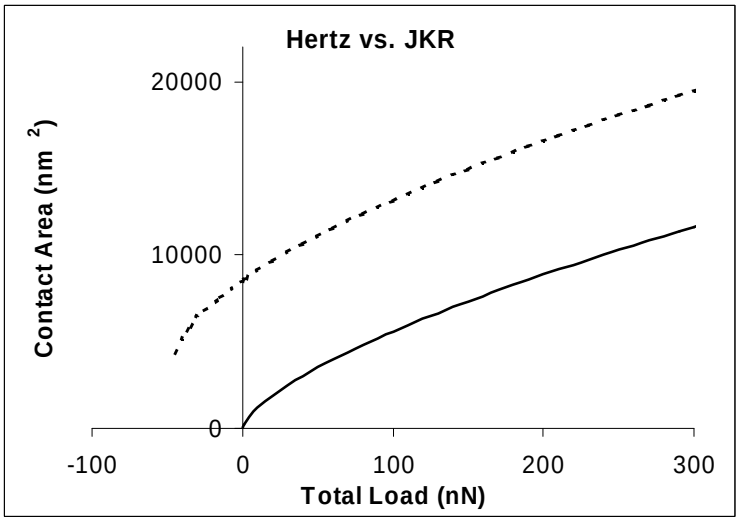

Figure 2: Hertzian elastic contact and JKR adhesive-elastic contact as function of load.

2. Force Modulation SFM and Hertzian Theory

The Hertzian theory of elastic circular point contact for a planar surface and an assumed spherically caped tip, Fig. 3, describes the contact radius as

$$a = \left[\frac{3LR}{4E}\right]^{1/3},$$

where R is the radius of curvature of the probing SFM tip, and E is the modulus of the sample only, if the sample material stiffness is much smaller than the modulus of the cantilever material. The mutual relative approach of distant points δ between the sample and probing tip, i.e., the sample indentation for an incompliant tip material, is given by the Hertzian theory as

$$\delta = \left[\frac{9L^2}{16RE}\right]^{1/3}$$

For a fully elastic sample and a incompliantly stiff probing SFM tip, δ reflects the elastic strain deformation (indentation) of the sample material. For a force modulated relative approach, the load varies around the equilibrium load L_o as

$$L = L_o + \frac{\partial L}{\partial \delta}\delta$$

As we consider only the sample being deformed, a one-dimensional sample stiffness (generally referred to as contact stiffness) can be introduced as the derivative of the load, i.e.,

$$k_c \equiv \frac{\partial L}{\partial \delta} = \left(6E^2 L_o R\right)^{1/3}.$$

The equation above is synonymous with the non-adhesive Hertzian expression

$$k_c = 2aE \,.$$

Higher order derivatives provide anharmonic distortions (dissipation) that can be neglected. The equilibrium load can be expressed by the normal spring constant of the cantilever k_L and the equilibrium deflection z_o as $L_o = k_L z_o$.

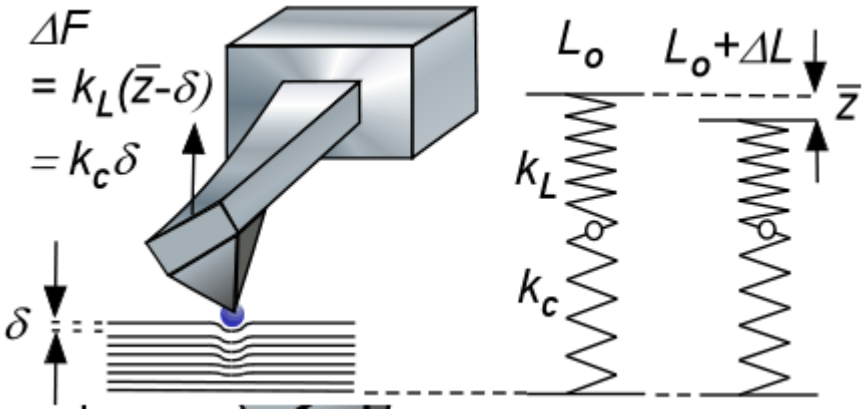

Figure 3: Elastic sample deformation involving rigid SFM tip.

Thus, for a sinusoidal normal stress disturbance, $z = A \sin(\omega t)$, with a root mean square amplitude

$$\bar{z} = \frac{1}{\sqrt{2}} A$$

the dynamic force acting on the cantilever is proportional to the net displacement (input modulation minus sample deformation), i.e.,

$$\Delta F = k_L \left(\bar{z} - \delta \right).$$

Analogous, the force modulation can also be described from the sample perspective as

$$\Delta F = k_c \delta \,.$$

The "normal force", ΔF, acting on the SFM lever in the process of an indentation can be expressed in Hooke's limit as

$$\Delta F = k_{sys} \bar{z} = k_c \delta = k_L \Delta z_L \quad \text{with} \quad \Delta z_L = \bar{z} - \delta \,,$$

as illustrated in Figure 3. The system combined spring constant, k_{sys}, is then given as

$$k_{sys} = \left(\frac{1}{k_c} + \frac{1}{k_L} \right)^{-1} \,.$$

Analogous relationships exist also for elastic shear modulation.

3. Contact Stiffness

In the previous paragraph, we have assumed that only the sample is deformed and the material response is rate independent. If both bodies are compliant, the non-adhesive Hertzian contact stiffness is given as

$$k_c = 2aE^* \text{ with } E^* = \left(\frac{1-\nu_1^2}{E_1} + \frac{1-\nu_2^2}{E_2} \right)^{-1}$$

where E_i and ν_i (I = 1,2) are the reduced material Young's moduli and Poisson ratios, respectively. This equation has also been found to be applicable for viscoelastic materials, i.e.,[1]

$$k_c(\omega) = 2aE^*(\omega).$$

where $k_c(\omega)$ and $E(\omega)$ reflect effective stiffnesses.

If we consider now also adhesion to take place in the contact area the Hertzian theory would have to be replaced by the JKR theory, which leads to the following expression for a normalized contact stiffness to zero load:[1]

$$\frac{k_c(\omega)}{k_c(\omega)\big|_{L=0}} = \left[\frac{1+\sqrt{1-L/F_{adh}}}{2} \right]^{2/3}, \text{ with}$$

$$k_c(\omega)\big|_{L=0} = 2a_o E^*(\omega) = 2E^*(\omega) \left[\frac{9\pi R^2 \Delta\gamma}{2E^*\big|_{\omega\to 0}} \right]^{1/3}$$

4. FM and Polymer Relaxation Properties

Controlled temperature experiments involving force modulation microscopy, provides the opportunity to investigate relaxation properties of polymeric and organic materials. Thereby, the contact stiffness is monitored as a function the temperature, as illustrated below with shear modulation force microscopy (SM-FM) employed to thin polystyrene films. Due to the small probing area even the smallest changes in the polymer internal pressure, modulus and surface energies can be detected. SM-FM is allows for accurate determination of transition properties, such as the glass transition temperature,* T_g, of nanoconstrained systems, such as ultrathin polymer films with a thickness below ~100 nm, Fig. 4(a).

The SM-FM method is briefly described as follows: A nanometer sharp SFM cantilever tip is brought into contact with the sample surface, Figure 4(b). While a constant load is applied, the probing tip is laterally modulated with a "no-slip" nanometer amplitude, ΔX_{IN}. The modulation response, ΔX_{OUT}, is analyzed using a two-channel lock-in amplifier, comparing the response signal to the input signal. The modulation response, i.e., the effective stiffness, is a measure of the contact stiffness. Thermally activated transitions in the material, such as the glass transition, T_g, are determined from the "kink" in the response curve, as shown in Figure 4(b).

Conceptually, the force modulation FM approach is a nanoscopic analogue to dynamic mechanical analysis (DMA). In essence, mechanical responses to external shear forces with varying temperature entail a material's viscoelastic properties, such as the modulus.

* Background information regarding the glass transition of viscoelastic material is provided below.

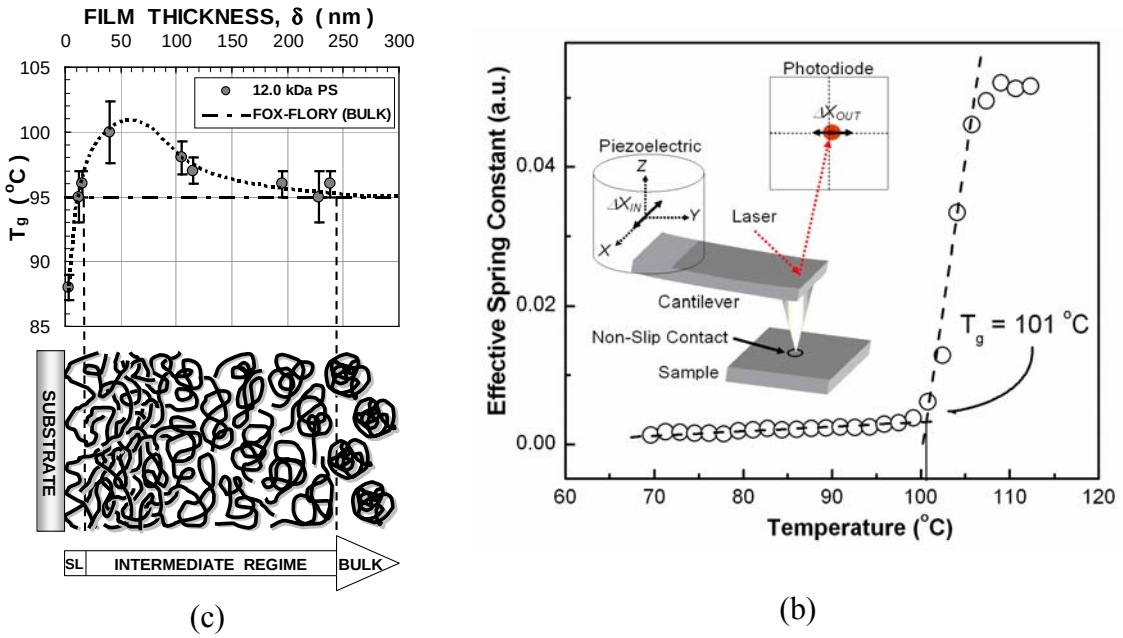

Figure 4. (a) Nanoscale constrained glass transition profile below 100 nm thick polymer films. (b)Working principle of Shear Modulation Force Microscopy (SM-FM)

5. Transition and Viscoelasticity

It is hard to imagine life without plastics, looking at water bottles, car bumpers, backpacks, computer casings, and many more products that involve synthesized organic materials – called polymers. There are numerous reasons to list why the last one hundred years can be called the *Plastic Age*. Polymers are light weight, formed in any shapes and colors, and can be produced with a simple scheme at low cost. One major advantage of polymers over traditional materials such as metals is their versatility in their mechanical property. Polymers can be soft and flexible like rubber bands and chewing gums, but also stiff and tough like the aircraft body of the new Boeing 787.

One critical parameter in designing polymeric product is the glass transition temperature T_g. The glass transition can be pictured, although with some caution, as a structural order-disorder transition that is observed in non-structured (amorphous) solids. One of the main features of the glass transition is the change in the mechanical and diffusive properties of the material below and above T_g. For instance, below T_g the material starts to act stiff and is brittle (i.e., glass like), and above T_g, still in the solid (condensed) phase, it exhibits high mechanical flexibility due to the existence of molecular chain mobility. Despite the importance of the glass transition of polymeric materials, the glass transition phenomena and its underlying viscoelastic behavior are not completely understood. These shortcomings have however not stopped mankind from designing continuously new polymer based products on a macroscopic level. However, the ambiguity in our current fundamental understanding of the glass forming process in polymers is being challenged by the recent nanotechnology spurt. As the dimension of solid systems approach the nanoscale, a dimension that is comparable to the size of polymer chains, it matters from an effective design perspective to grasp the exact relaxation mechanism behind the glass transition process.

One of today's most common ways to determine the glass transition temperature is the measurement of the change in the specific heat capacity $C_p(T)$ as a function of temperature by differential scanning calorimetry (DSC). Although widely used because of its convenience, DSC is also known for its inaccurately. One of the main reasons is that the glass transition process takes place not only at a specific temperature, like a typical first order phase transition, but over a range of temperatures[2]. Thus, T_g as determined by DSC has to be assigned, to some degree arbitrarily within a critical temperature range, as illustrated in Figure 5. Another reason for the difficulties in determine T_g originates from the viscoelastic nature of polymers, which makes the material temperature rate dependent with a high possibility of aging during the characterization process. DSC information is usually obtained from the polymer in powder form, to reduce effects based on thermal history and process engineered properties.[3] In other words for T_g determination, DSC is restricted to the characterization of bulk materials, like other widely used techniques, as the dynamic mechanical analysis (DMA), Fig. 5. DMA is sensitive to changes in the in-phase G' and out-of-phase modulus response G". The ratio of these two moduli components, define the loss modulus (also referred to as loss tangent tanδ), with which T_g can be identified. Due to imposed macroscopic mechanical constraints this value is often different from the DSC calorimetric glass transition.

There is currently not only a need for new techniques to provide a more fundamental understanding of the glass transition process, but also for methods that are applicable to small scale systems; e.g., thin films, and polymeric heterosystems (e.g., polymers blends and polymer nanocomposites). A technique that has been found to address the experimental shortcomings of DSC and DMA is shear modulation force microscopy (SM-FM), as introduced above.

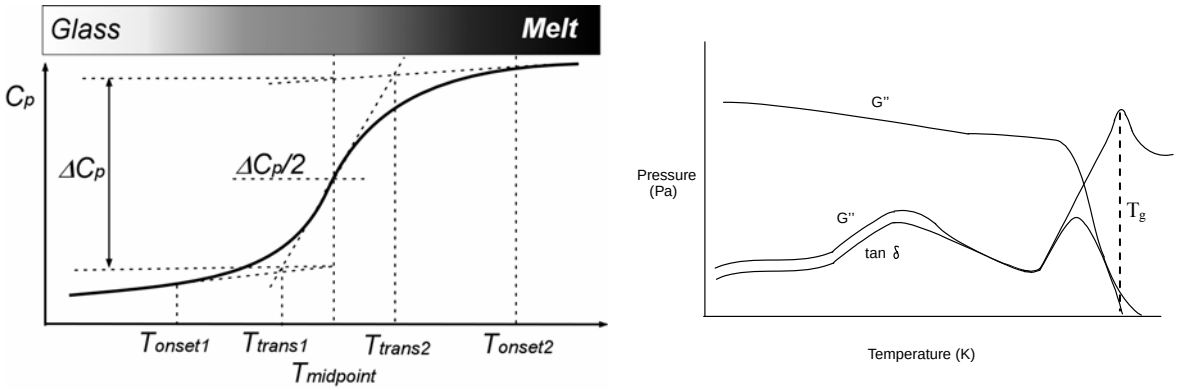

Figure 5 : (left) Schematic thermogram of $C_p(T)$. Shows the various distinct temperatures used to define the midpoint temperature T_g. (right) Schematic thermomechanical results, as obtainable by DMA.

6. Introduction to Linear Viscoelasticity

The science that deals with the mechanical properties of condensed phases under external stresses is called Rheology. We will limit our discussion to a subdiscipline of rheology, i.e., linear viscoelasticity, with which we conceptually separate the *liquid-like* (viscous) behavior from the *solid-like* (elastic) behavior. Thereby, a material that exhibits

ideal solid-like behavior under stress can be described with a simple stress-strain relationship, and a material with *ideal liquid-like* behavior shows a simple stress-strain-rate dependence. With *stress* we define the external force per unit area that is imposed on the condensed phase. The resulting deformation (e.g., length or angular deformation (ΔL or γ) for a uniaxial length extension, or simple shear, respectively) defines a strain ratio (e.g., $(L_o+\Delta L)/L_o$ or $\tan\gamma$). It is convention to use for uniaxial stress and strain the Greek symbols σ and ε and for the shear stress and strain τ and γ. Strain rates reflect the time derivative of the strain.

Ideal solid-like and ideal liquid-like

Ideal solid-like materials deform and relax instantaneously with changes in the applied external stresses. *Hooke's Law* is a manifestation of a solid-like behavior. Thus, an ideal solid-like behavior is synonymous with *ideal elastic*. Mechanical energy is stored in an ideal elastic material without exhibiting any form of energy dissipation. The energy is instantaneously regained with the discharge of the external stresses. Note, with this definition of a material behaving ideal solid-like, no structural arrangements, such as for instance "*crystallinity*", were imposed. In ideal elastic materials the stress is linearly related to the strain and the proportionality factor is called a *stiffness modulus*. In the case of a uniaxial elongation/compression in x-direction or simple shear in y-direction of an isotropic material, Hooke's law has the following simple form:

$$\sigma_{xx} = E\varepsilon_{xx} \quad \text{(unaxial deformation)}$$
$$\tau_{xy} = G\gamma_{xy} \quad \text{(simple shear deformation)}$$

with the modulus of elasticity (Young's modulus) E and the shear modulus G. The forces per unit area, i.e., $F_x/A = \sigma_{xx}$ and $F_y/A = \tau_{xy}$ are the normal and lateral stresses, respectively, which are imposed on the elastic solid. ε and γ are the corresponding strains; i.e., normalized dimensionless displacements.

The conceptual counter behavior to ideal solid-like is ideal liquid-like as found in a *Newtonian liquid*. The basic equation of simple flow is described one-dimensionally by *Newton's law of viscosity*,

$$\tau_{yx} = -\eta\frac{dv_x}{dy},$$

which relates proportionally the shear force per unit area, $F_x/A = \tau_{xy}$, to the negative of the local velocity gradient (time derivative of the deformation) with a constant viscosity value, η. The velocity gradient represents a strain rate. If a stress is applied to a Newtonian liquid no strain is built up. The material is incapable of mechanical energy storage. Once the stress is removed the material does not relax. The material resistance to shear manifests itself in the rate with which the stress is imposed. In a perfect liquid we find a linear relationship between the stress and the strain rate. The proportionality factor is called *viscosity*.

In general, any realistic liquid and solid matter will behave in a mixed manner, solid-like and liquid-like, depending on the degree and time scale over which external stresses are acting.

Linear Viscoelasticity

Mixed liquid-like and solid-like characteristics of viscoelastic materials suggest that the external forces applied are partially stored and partially dissipated. This is nicely described by a simple constitutive equation based on a periodic deformation process. If the viscoelastic behavior is in a linear region, a shear sinusoidal stress that is applied to a viscoelastic body exhibits a sinusoidal strain with a phase lag that is expressed as follows:

$$\gamma = \gamma_0 \sin(\omega \cdot t),$$

$$\sigma = \sigma_0 \sin(\omega \cdot t + \delta),$$

ω is the angular frequency, and δ is the phase lag, and γ_0 and σ_0 are the maximum magnitudes of the strain and the stress. The expression of the sinusoidal stress can be expanded to elucidate the two components, i.e., in phase component and out of phase component,

$$\sigma = \sigma_0 \sin(\omega \cdot t)\cos(\delta) + \sigma_0 \cos(\omega \cdot t)\sin(\delta).$$

The in phase component,t $\sigma_0 \cos(\delta)$ is referred to as the storage modulus *G'*, and the out of phase component, $\sigma_0 \sin(\delta)$ is called the loss modulus *G"*. The stress relationship then writes as

$$\sigma = \gamma_0 \cdot G' \cdot \sin(\omega \cdot t) + \gamma_0 \cdot G'' \cdot \cos(\omega \cdot t),$$

Expressed in complex notation the strain and stress are:

$$\gamma = \gamma_0 \exp(i \cdot \omega \cdot t),$$

$$\sigma = \sigma_0 \exp\left(i \cdot (\omega \cdot t + \delta)\right),$$

and thus, we can introduce a complex modulus *G** as,

$$\frac{\sigma}{\gamma} = G^* = \frac{\sigma_0}{\gamma_0}(\cos\delta + i \cdot \sin\delta) = G' + i \cdot G'',$$

The *storage modulus G'* represents the storage capability of the systems and the *loss modulus G"* describes the dissipation character of the system in form of plastic deformation or flow. The ratio of the loss and the storage component is referred to as the loss tangent,

$$\tan\delta = \frac{G''}{G'},$$

and reflects the relative viscous and elastic properties. The smaller the loss tangent is the more elastic is the material. tanδ is often the most sensitive indicator of various molecular motions within the material. Figure 6 provides a response visualization of a simple shear phenomenon.

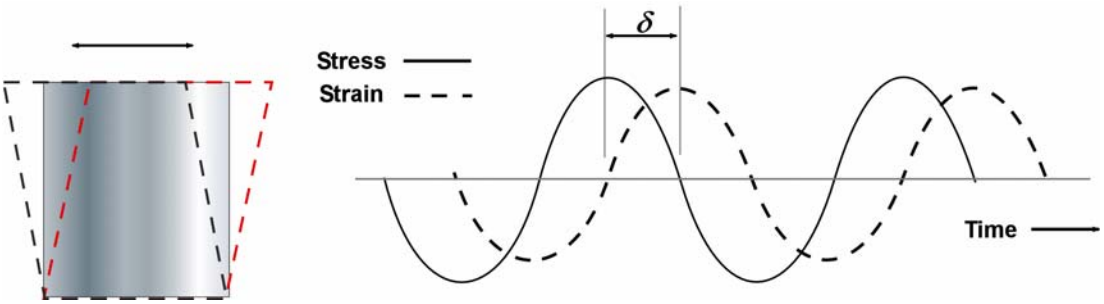

Figure 6: Dynamic shear stress-strain visualization.

The response of a viscoelastic material can be described by a simple combination of dashpots (dissipative) and springs (elastic). The simplest model of a spring and a dashpot in series is the Maxwell's model (Figure 7(a) with

$$\frac{d\gamma}{dt} = \frac{1}{G}\frac{d\sigma}{dt} + \frac{1}{\eta}\sigma$$

where η is the viscosity, we have introduced above. The solution to this differential equation is,

$$\sigma(t) = \gamma_0 \cdot G \cdot exp\left(-\frac{t}{\eta/G^*}\right)$$

with $G^* = \sigma/\gamma$. This model predicts a time sensitive modulus, i.e.,

$$G(t) = G \cdot exp\left(-\frac{t}{\tau_\gamma}\right),$$

where τ_γ is the characteristic relaxation time, and t is the observation time. Thus, if the deformation process is very fast compared to the material relaxation time, i.e., $t \gg \tau_\gamma$ the elastic behavior will dominate. For very slow deformation ($t \ll \tau_\gamma$), the system's viscous behavior dominates. Another basic viscoelastic setup is obtained by operating a spring in parallel with a viscous dashpot. (Kelvin-Voigt Model,Fig. 2(b))The Kelvin-Voigt model provides the following relationships:

$$\sigma = G \cdot \gamma + \frac{\eta \cdot d\gamma}{dt}$$

and the solution with a constant stress σ_0 is,

$$\gamma(t) = \frac{\sigma_0}{G}\left[1 - exp\left(-\frac{t}{\tau_\sigma}\right)\right]$$

where τ_σ is the retardation time of the strain.

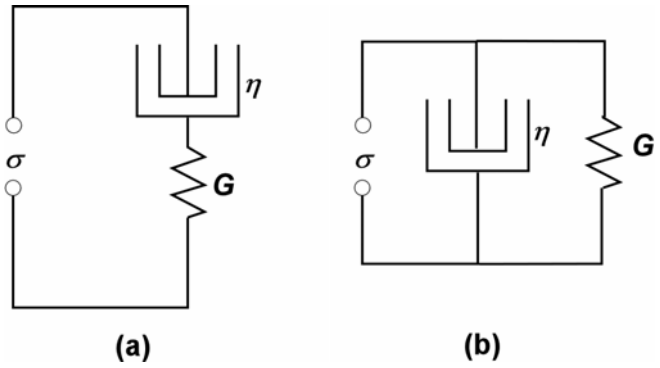

Figure 7: Dashpot spring model of (a) Maxwell Model (b) Kelvin-Voigt Model.

While the Maxwell model describes the stress relaxation but not creep, the Kelvin-Voigt model describes creep but not stress relaxation. For viscoelastic material, the simplest model would be the combination of the two, [4]

$$\sigma + \left(\frac{\eta_1 + \eta_2}{G_1} + \frac{\eta_2}{G_2}\right)\frac{d\sigma}{dt} + \frac{\eta_1\eta_2}{G_1G_2}\frac{d^2\sigma}{dt^2} = \eta_2\frac{d\gamma}{dt} + \frac{\eta_1\eta_2}{G_1}\frac{d^2\gamma}{dt^2}$$

as G_1, G_2, η_1 and η_2 are corresponding to two springs and two dashpots, Fig. 8. If this is solved with the sinusoidal stress,

$$\frac{G'-G_0}{G_\infty - G_0} = \frac{\omega^2 \cdot \tau_\gamma^2}{1+\omega^2 \cdot \tau_\gamma^2}$$

$$\frac{G''}{G_\infty - G_0} = \frac{\omega \cdot \tau_\gamma}{1+\omega^2 \cdot \tau_\gamma^2}$$

$$\tan\delta_m = \frac{G_\infty - G_0}{G_0 + G_\infty \omega^2 \cdot \tau_m^2}$$

where G_0 and G_∞ are *relaxed* and *unrelaxed* moduli, respectively, and τ_m is derived as:

$$\tau_m = (\tau_\sigma \tau_\gamma)^{1/2} = \left(\frac{\eta_1}{G_1} \frac{\eta_1}{G_1 + G_2} \right)^{1/2}$$

The maximum of the loss curve then corresponds to $\tau_m \omega_0 = 1$. The product $\tau_m \omega_0$ is referred to in the literature as the Deborah number, and reflects the ratio of the externally imposed time disturbance and the intrinsic relaxation time[4]

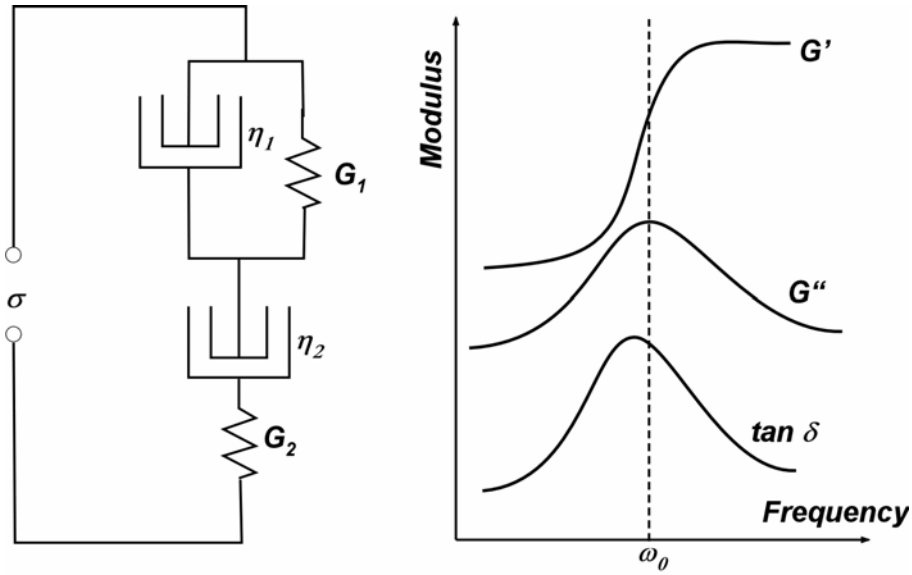

Figure 8: A combination of the Maxwell and Kelvin-Voigt Model.

Many more combinations of springs and dashpots are possible and in detail described in the literature.[3]

7. Time-Temperature Equivalence of Viscoelastic Behaviors

We showed in the previous section that the viscoelastic behavior is strongly affected by the temperature and the observation time (frequency). Here the concept of time-temperature equivalence is introduced. Consider a glass window. Glass windows are made with an amorphous inorganic (silica mixture) material that appears in daily life to be "solid-like. However, it is more appropriate to consider glass to be in a highly viscous condensed phase that appears to be at equilibrium in a solid-like state during the

time of observation. By controlling the temperature without imposing any transitions we can accelerate or slow down the flow process In that sense, the viscoelastic behavior of the material is affected similarly by either changes in the temperature and or time. This is called a time-temperature equivalence and is illustrated in Figure 9. Figure 9(a) and 9(b) reflect the modulus in a time (i.e., frequency) domain, and in a temperature domain, respectively. Valuable information about the viscoelastic behavior of materials can be deduced from such measurements and will be discussed in the following sections.

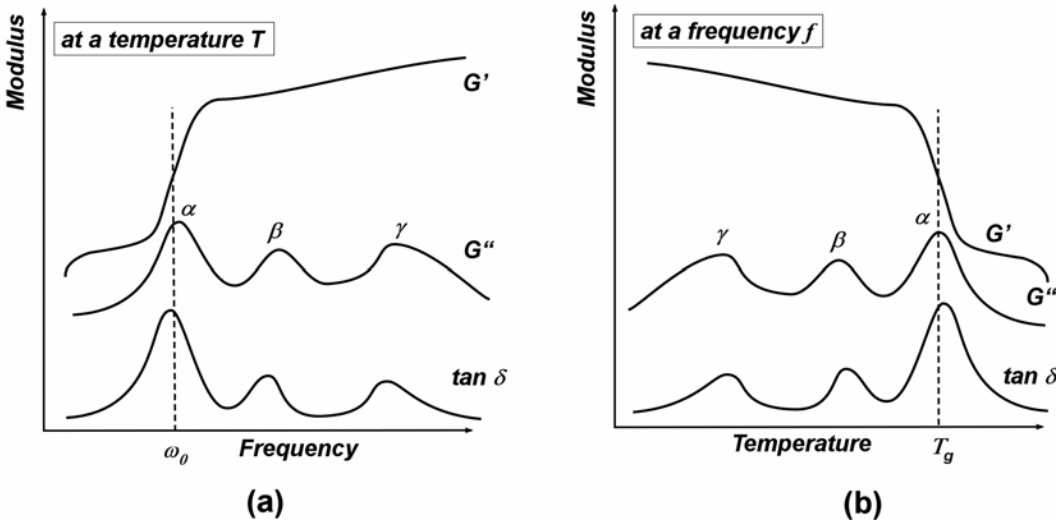

Figure 9: Modulus spectrums in (a) time domain, and in (b) temperature domain.

8. Glass Transition

The *glass transition* T_g is defined as the reversible change in an amorphous material (e.g., polystyrene) or in amorphous regions of a partially crystalline material (e.g., polyethylene), from (or to) a viscous or rubbery condition to (or from) a hard and relatively brittle one.[5] As shown in the previous section, Fig. 9(b), this transition corresponds to a temperature at which the modulus drastically changes. Above the glass transition temperature the material, still a solid, reveals a strongly rubbery behavior that is to part liquid-like. Below the transition temperature the material behaves like a brittle solid-like material. The glass transition itself, as illustrated in Figure 10, exhibits a strong cooling rate dependence and is in appearance significantly different from melting (first order phase) transition. Also the frequency of the applied macroscopic stresses is affecting the temperature of the transition.

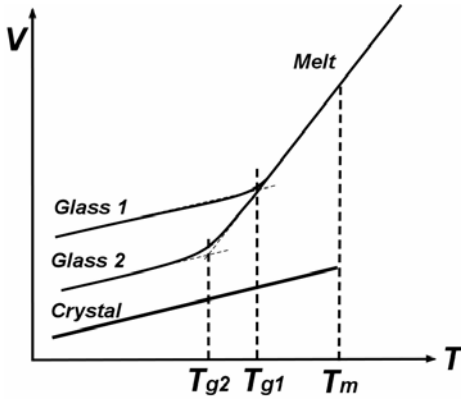

Figure 10: Specific volume change as function of temperature. Depending on the cooling rate any liquid can freeze into a glass phase (fast quenching; e.g. of metallic glasses). Depending on the cooling rate, T_g can significantly shift as indicated with Glass 1 and Glass 2. In polymers, the transition from a melt to a glass is not discontinuous as the first order phase transition (indicated with melting temperature T_m). Hence the assignment of a single transition value for T_g seems to be ambiguous on first sight.

Thermodynamically, the free energy changes between equilibrium states are usually identified by a discontinuity in the first partial derivatives of the Gibbs free energy G = H -TS, with respect to the relevant state variable (pressure P and temperature T), as illustrated Figure 11. Discontinuities, as expressed in the first partial derivatives of the Gibbs free energy

$$\left(\frac{\partial G}{\partial P}\right)_T = V ,$$

$$\left(\frac{\partial G}{\partial T}\right)_P = -S ,$$

$$\left(\frac{\partial (G/T)}{\partial (1/T)}\right)_P = H ,$$

are found in the property-temperature relationships, i.e., the volume V, the entropy S and enthalpy H.

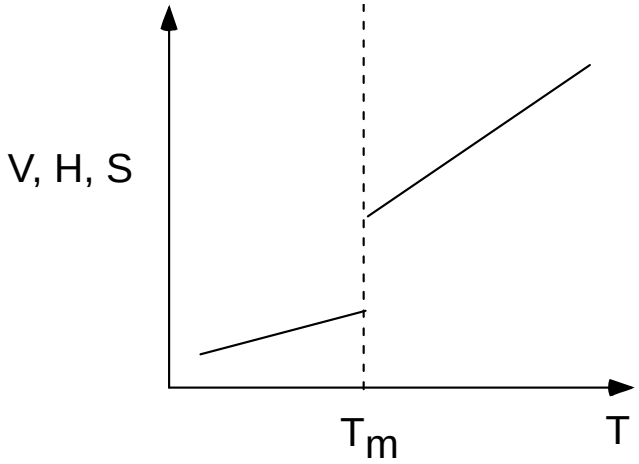

Figure 11: Volume discontinuity. First-order transition between liquid and solid. (T_m melting temperature).

The second derivatives of the Gibbs free energy introduces the heat capacity C_p, compressibility κ and thermal expansion coefficient α.

Heat Capacity, C_p : $$-\left(\frac{\partial^2 G}{\partial T^2}\right)_P = \left(\frac{\partial S}{\partial T}\right) = \frac{C_p}{T}$$

$$\frac{\partial}{\partial T}\left[\left(\frac{\partial (G/T)}{\partial (1/T)}\right)_P\right]_P = \left(\frac{\partial H}{\partial T}\right)_P = C_P$$

Compressibility, κ: $$\left(\frac{\partial^2 G}{\partial P^2}\right)_T = \left(\frac{\partial V}{\partial P}\right)_T = -\kappa V$$

Therm. Expansion Coeff., α: $$\left[\frac{\partial}{\partial T}\left(\frac{\partial G}{\partial P}\right)_T\right]_P = \left(\frac{\partial V}{\partial T}\right)_P = \alpha V$$

Figure 12 provides a rough classification based on the changes of the free energy and derivatives with temperature. While, column (i) illustrates the qualitative behavior of a first-order phase transition (i.e., a melting/freezing transition), column (ii) and (iii) are found for second order and glass transitions, respectively. A second order phase transition (e.g., an order-disorder transition) exhibits no discontinuity in *V* and *H*, and *S*. But there are discontinuities in C_p, κ and α.

First and second order transitions are illustrated in Figure 12. If compared to property changes in glasses around the glass transition temperature, one finds some similarity between the glass transition and the second order transition. There are however significant differences. C_p, κ and α values are always smaller and closely constant below the glass transition temperature, T_g, if compared to the values above T_g. This is in contrast to the second-order transition.

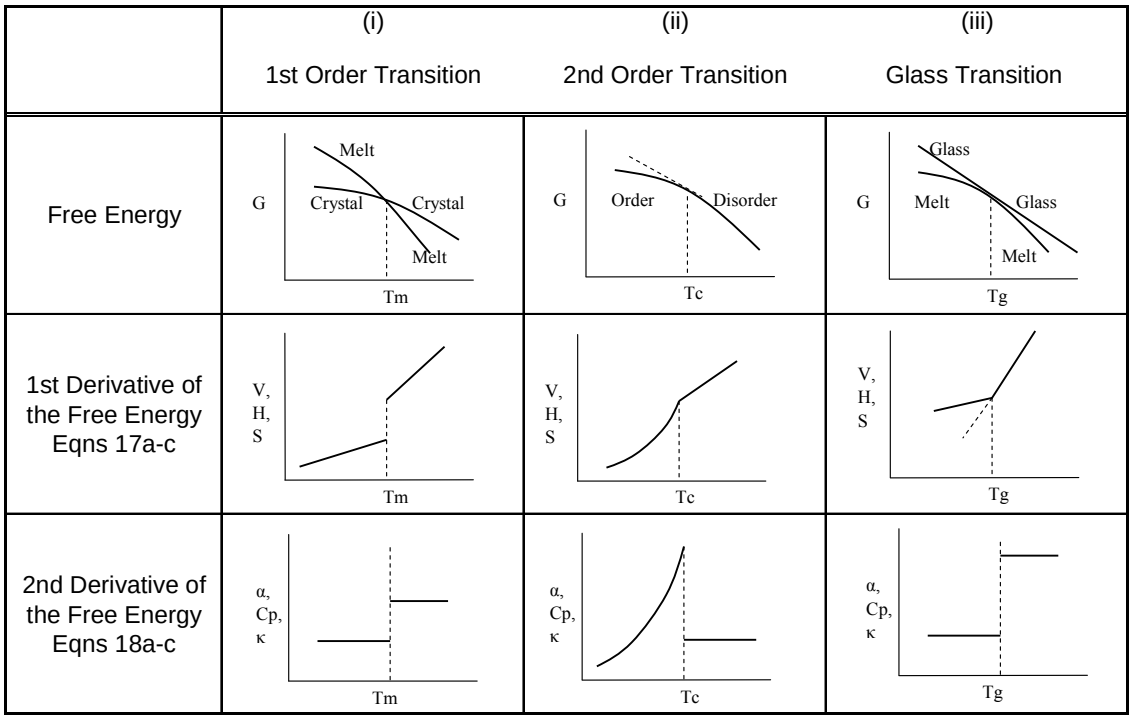

Figure 12: Schematic representation of the changes with temperature of the free energy and its first and second derivatives for (i) first order, (ii) second order and (iii) glass transition.

References

1. D.M. Ebenstein and K. J. Wahl, Coll. Interf. Sci. **298**, 652 (2006).
2. J. J. Aklonis and W. J. MacKnight, *Introducrtion to polymer viscoelasticity*, 2nd ed. (Wiley-Interscience Publication, New York, 1983).
3. D. W. Van Krevelen, *Properties of polymers*. (Elsevier Scienfitic Publishing Company, Amsterdam, 1976).
4. P. Hedvig, *Dielectric spectroscopy of polymers*. (John Wiley & Sons, New York, 1977).
5. A. S. f. T. M. A. E1142.
6. T. G. Fox and P. J. Flory, J. Appl. Phys. **21**, 581 (1950).
7. C. Buenviaje, F. Dinelli, and R. M. Overney, in *American Chemical Society Symposium Series*, edited by J. Frommer and R. M. Overney (University Press, 2000).

Recommended Reading

Introduction to Polymer Viscoelasticity by John J. Alkonis and William J. MacKnight, Wiley-Interscience Publication, 2nd Ed., New York, 1983.

Mechanical Properties of Solid Polymers by I. M. Ward, Wiley-Interscience Publication, London, 1971.

Nanoscience: Friction and Rheology on the Nanometer Scale by E. Meyer, R. M. Overney, K. Dransfeld, and T. Gyalog, World Scientific Publ., Singapore, 1998.